

## WSS25 INHIBITS GROWTH OF XENOGRAFTED HEPATOCELLULAR CANCER CELLS IN NUDE MICE BY DISRUPTING ANGIOGENESIS VIA BLOCKING BMP/SMAD/ID1 SIGNALING

Hong Qiu (邱宏)<sup>1</sup>, Bo Yang (杨波)<sup>2,§</sup>, Zhi-Chao Pei (裴志超)<sup>1,§</sup>, Zhang Zhang (章漳)<sup>1</sup>, Kan Ding (丁侃)<sup>1,3</sup>

From <sup>1</sup>Glycochemistry & Glycobiology Lab, Shanghai Institute of Materia Medica, Chinese Academy of Sciences, Shanghai 201203, China.

<sup>2</sup>College of Pharmaceutical Sciences, Zhejiang University, Hangzhou 310058, China.

<sup>3</sup>Joint Laboratory for The Research of Chinese Herbal Polysaccharides -Shanghai Institute of Materia Medica, Chinese Academy of Sciences and Infninitus.

**Running title:** Targeting BMP/Smad/Id1 signaling to disrupt angiogenesis

**Address correspondence to:** Kan Ding, Ph.D, 555 Zuchongzhi Road, Zhangjiang High-Tech Park, Shanghai, China. Fax: +86-2150806928; E-mail: [kding@mail.shcnc.ac.cn](mailto:kding@mail.shcnc.ac.cn).

The highly expressed Id1 (inhibitor of DNA binding/differentiation) protein promotes angiogenesis in HCC and is a well-established target for anti-angiogenesis therapeutic strategies. Heparan sulphate (HS) mimetics such as PI-88 can abrogate HS-protein interactions to inhibit angiogenesis. Id1 is the direct downstream effector of BMPs (Bone morphogenetic proteins), which are angiogenic and HS binding proteins. Thus, targeting BMPs by HS mimetics may inhibit angiogenesis via attenuating Id1 expression. We report here that a HS mimetic WSS25 potently inhibited the tube formation of HMEC-1 cells on Matrigel and their migration. Meanwhile, WSS25 (25 µg/mL) nearly completely blocked Id1 expression in the HMEC-1 cells as demonstrated by oligo-angiogenesis microarray analysis and further confirmed by RT-PCR and Western blotting. The BMP/Smad/Id1 signaling was also blocked by WSS25 treatment in the HMEC-1 cells. Importantly, Id1 knock-down in HMEC-1 cells caused the disruption of their tube formation on Matrigel. By employing quartz crystal microbalance (QCM) analysis, we found that WSS25 strongly bound to BMP2. Moreover, WSS25 impaired BMP2 induced tube formation of HMEC-1 cells on Matrigel and angiogenesis in Matrigel transplanted into C57BL6 mice. Furthermore, WSS25 (100 mg/kg) abrogated the growth of HCC cells xenografted in male nude mice. Immunohistochemical analysis showed that both the expression of Id1 and the endothelial cell marker CD31 were lower in the WSS25 treated tumor tissue than in the control.

Therefore, WSS25 is a potential drug candidate for HCC therapy as a tumor angiogenesis inhibitor.

HCC is the 4<sup>th</sup> leading cause of deaths from cancer worldwide and the 2<sup>nd</sup> most lethal malignant cancer in China since the 1990s (1). However, there are few treatment options aside from surgery (1). HCC is characterized by hypervascularity, which can distinguish HCC from benign lesions by angiography. The strategy of blocking angiogenesis in HCC to inhibit tumor growth has been used for over 20 years in the clinic (2). However, there are no ideal anti-angiogenesis chemotherapeutic agents developed thus far for HCC therapy.

Id1 is one of the inhibitors of DNA binding proteins (Ids) which belongs to the bHLH transcriptional factor superfamily (3). There are four members, Id1, Id2, Id3, and Id4 in the Ids family. Accumulating evidence show that Id1 is over-expressed in solid tumors and their supporting vasculatures (4, 5). Although essential during embryo development, Id1 expression is extremely low in adult tissues including the quiescent endothelial cells (6). Partial loss of Id1 by genetic manipulation in mice effectively inhibits tumor angiogenesis (6). Id1 ablation leads to the impairment of bone marrow endothelial progenitor cell recruitment and mobilization to form tumor vasculature (7, 8). Id1 has also been implicated in the regulation of cell senescence, drug resistance, tumor cell invasion, and apoptosis resistance (9). Interestingly, Id1 has been demonstrated to be highly expressed in malignant HCC and to promote angiogenesis in HCC (10,11). Thus, Id1

is a rational target for the development of anti-angiogenesis therapeutics for HCC.

Heparan sulphate proteoglycans (HSPGs) are glycoconjugates composed of protein cores to which heparan sulphate (HS) chains are attached. Direct genetic evidence supports that HSPGs are necessary for tumor angiogenesis (12). HSPGs, especially those located on the cell surface, act as co-receptors through their HS chains (13). HS chains are negatively charged polymers composed of hexaronic acid and glucosamine disaccharide repeats. Due to their negative charge, they bind multiple functional proteins including pro-angiogenic factors such as VEGF, FGF2, and thus mediate angiogenic signaling (14). HS mimetics such as PI-88 can inhibit angiogenesis via disrupting those interactions between HS and growth factors (15). TGF- $\beta$  family proteins can also bind HS chains. The binding is isoform-specific and the established examples include BMP2 (16) and BMP4 (17), two angiogenic factors (18) and the upstream molecules of the BMP/Smad signaling pathway (19), while Id1 is a canonical and direct downstream effector of this pathway (20). More importantly, stimulation of Id1 expression by BMP proteins is sufficient and necessary for activating endothelial cells (21). Id1 is also the downstream effector of VEGF and FGF2 signaling pathway (3, 22). Moreover, targeting the HS-protein interaction is a new approach for drug design (23). Therefore, we hypothesized that HS mimetics may inhibit angiogenesis through blocking BMP-induced Id1 expression. We previously isolated an alpha-D-(1-4) glucan with an alpha-D-(1-4) branch periodically at O-6 from a well-known Chinese herb *Gastrodia elata* Bl. WSS25 (Fig. 1) is a sulfated derivative of the aforementioned glucan and a HS mimetic (24). In this study, we investigated the role of WSS25 on angiogenesis, Id1 expression, BMP2 induced BMP/Smad/Id1 signaling, and growth of HCC.

## EXPERIMENTAL PROCEDURES

*General materials-* WSS25 was prepared in our lab as described previously (24) and dissolved in normal saline for experimental use after passing through a 0.22  $\mu\text{m}$  filter. Matrigel with growth factors and reduced growth factors were obtained from BD Biosciences (Bedford, MA, U.S.A.). The proteinase inhibitor cocktail and actin primary antibody were from Sigma-Aldrich (St. Louis, MO, U.S.A.). Fetal bovine

serum (FBS) was from Sijiqing Co. Ltd. (Hangzhou, China). Other antibodies used include the Id1 antibody (c20) (Santa Cruz, USA), phosphorylated Smad1/5/8 primary antibody (Cell Signaling Technology, U.S.A.), HRP conjugated anti-rabbit & anti-mouse secondary antibody (Jackson ImmunoResearch Laboratories, U.S.A.), anti-CD31 (Boster Biological Technology, Ltd. Wuhan, China), Ki-67 antibody (Abcam, San Francisco, CA, U.S.A.), and anti-TUNEL antibody (Trevigen Inc., Gaithersburg, MD, U.S.A.). Other reagents, unless specified, were obtained from Sinopharm Chemical Reagent Co. Ltd (Shanghai, China).

*Cell lines and cell culture-* Human microvascular endothelial cells (HMEC-1) (25) were maintained in MCDB131 (Gibco BRL, U.S.A.) medium containing 15% FBS (v/v), 2 mM L-glutamine, 10 ng/mL EGF (Shanghai PrimeGene Bio-Tech Co., Ltd., Shanghai, China) and antibiotics (100 U/mL penicillin, 100  $\mu\text{g}/\text{mL}$  streptomycin, Gibco BRL, U.S.A.). SMMC7721 and Bel7402 cells (both from the Cell Bank in the Type Culture Collection Center in Chinese Academy of Sciences, Shanghai, China) were cultured in RPMI1640 media supplemented with 10% FBS and antibiotics. All cells were cultured in a humidified incubator at 37°C with 5% CO<sub>2</sub>.

*Tube formation assay-* The tube formation assay was performed to determine the effect of WSS25 on angiogenesis *in vitro*. Briefly, a 96-well plate coated with 50  $\mu\text{L}$  Matrigel per well was allowed to solidify at 37°C for 30 min. HMEC-1 cells ( $3 \times 10^4$  cells/well) were seeded into the plate and cultured in MCDB131 media containing 6.25  $\mu\text{g}/\text{mL}$ , 25  $\mu\text{g}/\text{mL}$  or 50  $\mu\text{g}/\text{mL}$  of WSS25 for 10 h. For the BMP2 (Shanghai PrimeGene Bio-Tech Co., Ltd., Shanghai, China) induced tube formation in FBS restricted conditions (0.1% FBS in MCDB131 medium), BMP2 dissolved in 10 mM HAc (200 ng/mL) with or without WSS25 (25  $\mu\text{g}/\text{mL}$ ) was added to the cells on the growth factor reduced Matrigel in the 96-well plate, with 10 mM HAc as the control. Noggin (Shanghai PrimeGene Bio-Tech Co., Ltd., Shanghai, China) was also dissolved in 10 mM HAc (1  $\mu\text{g}/\text{mL}$ ) and added into the cells together with BMP2 (200 ng/mL) as aforementioned. The enclosed capillary networks of tubes were photographed by a microscope (Olympus, IX51, Japan).

*Migration assay-* The migration assay was performed by using a 24-well chamber (Costar, Cambridge, MA, U.S.A.) as the outer chamber and polycarbonate filters (8  $\mu\text{m}$  pores) as the

inner chambers. HMEC-1 cells ( $1.5 \times 10^5$  cells/well) were seeded into the inner chamber in MCDB-131 medium containing WSS25 or vehicle (control). The outer chamber contained the same medium with 15% FBS. After incubation for 14 h at 37°C, the cells on the filter were fixed in 90% ethanol for 10 min. Non-migrated cells on the upper surface of the filter were removed by gentle scraping with a cotton swab. Migrated cells on the lower surface of the filter were stained with 0.1% crystal violet and washed with distilled water until the water was colorless. Images of migrated cells were captured using a microscope (Olympus, IX51, Japan) and measured at 595 nm after extraction with 10% acetic acid.

*Wound healing assay*- HMEC-1 cells ( $5 \times 10^5$  cells per well) were seeded into a 6-well plate. A wound in each well was created by scratching with a yellow tip after incubation for 24 h. After rinsing with PBS three times, the cells were incubated with new medium containing WSS25 (25  $\mu$ g/mL) or the vehicle. Photos were taken immediately or 48 h later under a microscope (Olympus, IX51, Japan). The distance of the wound was calculated by ImageJ.

*MTT assay*- HMEC-1 cells ( $4.5 \times 10^3$  cells/well) were seeded into the 96-well plate for 24 h before WSS25 was added into the plate. After treatment with WSS25 for 24 h, 48 h or 72 h, Thiazolyl Blue Tetrazolium Bromide (5 mg/mL) (MTT, Sigma-Aldrich, St. Louis, MO, U.S.A.) was then added to each well and incubated for 4 h. The formazan crystals formed from MTT by the living cells were dissolved in the lysis buffer (10% SDS; 5% isopropanol; 0.1M HCl) for 12 h, and the purple solution of the formazan was detected using a spectrophotometer at 570 nm. The inhibitory ratio was calculated as [(control-sample) / control]  $\times$  100%.

*Oligo angiogenesis array analysis*- Total cellular RNA was extracted from HMEC-1 cells using Trizol (Invitrogen, Carlsbad, CA, U.S.A.). RNA was quantified by using the Nanodrop ND-1000. Using the True-Labeling AMP Linear RNA amplification kit (SuperArray Bioscience Corporation, Frederick, MD, U.S.A.), the mRNA was reverse transcribed to obtain cDNA and converted into biotin-labeled cRNA using biotin-16-dUTP (Roche, U.S.A.) by *in vitro* transcription. Before hybridization, the cRNA probes were purified with an ArrayGrade cRNA cleanup kit (SuperArray Bioscience Corporation, Frederick, MD, U.S.A.). The purified cRNA

probes were then hybridized to the pre-treated Oligo Human Angiogenesis Arrays (SuperArray Bioscience Corporation, Frederick, MD, U.S.A.), which covers 114 angiogenesis-related genes plus controls (Supplemental file 1). After the washing steps, array spots with bound cRNA were detected by the chemiluminescence method according to the manufacturer's procedure. Spots were then analyzed by using the GEArray Expression Suite (SuperArray Bioscience Corporation, Frederick, MD, U.S.A.). All genes covered in the array can be found at the website of SuperArray Bioscience.

*RT-PCR*- Total RNA was extracted using Trizol reagent (Invitrogen, U.S.A.) according to the manufacturer's manual after WSS25 treatment for 18 h. First-strand cDNA was synthesized from 1  $\mu$ g total RNA using avian myeloblastosis virus reverse transcriptase (AMV-RT, Takara, Dalian, China) according to the manufacturer's instructions. The primers and conditions for Id1 were the same as that used by Peddada et al. (26) or McAllister et al. (27). The PCR primers and conditions for BMP2, BMPRIA, BMPRIB, BMPRII, and Smad4 were also previously published (28).

*Western blotting analysis*- HMEC-1 cells were seeded ( $5 \times 10^5$  cells / well) into 6-well plates. Cells treated under different conditions were lysed with an equal volume of RIPA buffer (0.5% Triton-X 100, 0.5% deoxycholic acid sodium salt, 0.1% SDS and 1% PMSF supplemented with 1% proteinase inhibitor cocktail). Protein concentrations were determined by a protein assay according to the manufacturer's instructions (BioRad, U.S.A.). The proteins were separated by SDS-polyacrylamide gel electrophoresis and transferred to a polyvinylidene difluoride (PVDF) membrane (BioRad, U.S.A.). After blocking with TBST containing 5% non-fat milk for 30 min, the membrane was incubated with antibodies against actin, Id1 and phospho-Smad1/5/8 (ser463/465) overnight at 4°C. After incubation in horseradish peroxidase-conjugated secondary antibody for 1 h, Pierce ECL Western Blot Substrate (Pierce, U.S.A.) was used for detection.

*Gene knock-down using shRNA*- The sequences for the Id1 shRNA and negative control were 5'-cac cgc cca ttt ctg ttt cag cca gtt tca aga gaa ctg gct gaa aca gaa tgg gct ttt ttg-3', and 5'-cac cgt tct ccg aac gtg tca cgt caa gag att acg tga cac gtt cgg aga att ttt tg-3', respectively. HMEC-1 cells ( $2.5 \times 10^5$  cells/well) were seeded

into 6-well plate 24 hours before transfection. The plasmids (the vector is pGPU6/GFP/Neo) were transfected into the cells three times 24 h apart using the X-fect polymer (Clontech, U.S.A.) according to the instructions from the company. After another 24 h of incubation, the cells were used in the tube formation assay as described above. The shRNA plasmids were from Shanghai GenePharma Co., Ltd., Shanghai, China.

**Quartz crystal microbalance (QCM) analysis-** Biotinylated WSS25 was synthesized by adding Biotin-PEG4-hydrazide (50  $\mu$ L, 50 mM) in a water-miscible solvent (H<sub>2</sub>O:DMSO, 4:1) to WSS25 (450  $\mu$ L, 31  $\mu$ M) in the coupling buffer (0.1 M sodium phosphate, 0.15 M NaCl, pH 7.2), and the mixture was stirred at room temperature for 2 h. The biotinylated WSS25 was purified from non-reacted biotin reagent by using a desalting column. To measure carbohydrate-protein interactions, biosensor experiments were carried out on an Attana A100 QCM instrument (Attana AB, Stockholm, Sweden). The Attana biotin sensor surfaces were mounted in the QCM system and equilibrated with buffer solution (10 mM Hepes, 150 mM NaCl, 0.005% Tween 20, pH 7.4). Subsequently the streptavidin solution (100  $\mu$ g/mL) was injected, and the biotinylated WSS25 was immobilized on the streptavidin surface to produce a WSS25 biosensor surface. The interaction between WSS25 and BMP2 were then measured by injecting BMP2 (50  $\mu$ g/mL, 50  $\mu$ L) in running buffer (10 mM Hepes, 150 mM NaCl, 0.005% Tween 20, pH 7.4) onto the WSS25 biosensor surface, and frequency data were collected. A continuous flow of running buffer at a flow rate of 25  $\mu$ L/min was used throughout, and the samples were prepared in the same buffer. The frequency responses produced from the interactions were monitored by frequency logging with Attester 1.1 (Attana), where the mass changes from the bound or released ligands were recorded as the resulting frequency shifts ( $\Delta$ f).

**Animals-** All mice were housed in sterile cages within laminar air flow hoods under specific pathogen-free conditions with sterile food and water *ad libitum*. All animal experiments were performed according to a protocol approved by the Institutional Animal Care and Use Committee.

**Matrigel plug assay-** Human recombinant BMP2 protein was mixed with growth factor reduced Matrigel via vortexing, at the ratio of 4

$\mu$ g protein per 1 mL Matrigel. The mixture was injected subcutaneously into the ventral region of the female C57BL6 mice ages 4–6 weeks, and 0.1% BSA served as a control. The mice were randomly grouped, five mice for each group. WSS25 (25 mg/kg and 100 mg/kg) and normal saline (vehicle) were administered subcutaneously every other day for 10 times from the second day after injecting the Matrigel. The mice were then sacrificed and followed by excision of the Matrigel plug, and photographs were taken.

**Tumor xenograft experiment-** Bel7402 cells ( $1 \times 10^6$  cells/mouse) or SMMC7721 ( $1 \times 10^7$  cells/mouse) cells were subcutaneously injected into BALB/cA nu/nu male mice ages 4 to 6 weeks. For the Bel7402 tumor xenografts, as the tumor volume reached around 100 mm<sup>3</sup>, the mice were randomly assigned into control and treatment groups (5 mice/group). For the SMMC7721 tumor xenografts, well-developed tumors were cut into 1-3 mm<sup>3</sup> fragments and transplanted subcutaneously into the right flank of nude mice using a trocar under sterile conditions. When the tumor volume reached around 100 mm<sup>3</sup>, the mice were randomly assigned into control and treatment groups (6 mice/group). The vehicle (normal saline) or 100 mg/kg body weight of WSS25 was administered via tail vein injection every other day.

**Measurement of the tumor volume-** The tumor volume (V) was calculated as follows:  $V = (\text{length} \times \text{width}^2) / 2$ . The individual relative tumor volume (RTV) was calculated as follows:  $\text{RTV} = V_t/V_0$ , where  $V_t$  is the volume on each day, and  $V_0$  is the volume at the beginning of the treatment. The therapeutic effect of the compounds was expressed as the volume ratio of treatment to control (T/C).  $T/C (\%) = 100\% \times (\text{mean RTV of the treated group} / \text{mean RTV of the control group})$ .

**Immunohistochemistry-** At the end of the experiment, the mice were sacrificed and the tumor tissues were excised, fixed in 4% neutral paraformaldehyde and embedded in paraffin. After sectioning, the 5  $\mu$ m tissues were deparaffinized by xylene, ethanol, 95% ethanol, 80% ethanol sequentially. The endogenous peroxidase was removed by incubating with 3% H<sub>2</sub>O<sub>2</sub> at room temperature for 10 min. The retrieval of antigen was performed by boiling the tissue in citrate buffer at pH 6.0 for 3 times, each with a 10 min interval. The tissue was sequentially probed with primary antibodies against CD31 (1:10), phosphorylated Smad1/5/8

(1:100) or Id1 (1:100) overnight at 4°C. After application of the anti-rabbit/anti-mouse secondary antibody and appropriate washes, the signals were detected by staining the sections with 3,3'-diaminobenzidine (DAB) and counterstaining with hematoxylin.

*Statistical analysis*- Results were expressed as the mean  $\pm$  the standard error of the mean (SEM). The data was analyzed by the Student's *t* test; *P* values of  $< 0.05$  indicated significant differences (\* *P*  $< 0.05$ ; \*\* *P*  $< 0.01$ ).

## RESULTS

*WSS25 inhibits the tube formation of HMEC-1 cells on Matrigel and migration.* As HS mimetics have the potential to inhibit angiogenesis, we first tested whether WSS25 in different concentrations also has this impact on angiogenesis *in vitro*. Therefore, the tube formation of HMEC-1 cells on Matrigel, a typical *in vitro* angiogenesis model, was employed (29). The results showed that WSS25 at 25 or 50  $\mu\text{g/mL}$  almost completely disrupted the enclosed capillary networks (c, d, respectively in Fig. 2A) formed by the HMEC-1 cells (a, in Fig. 2A), while little effect was observed at 6.25  $\mu\text{g/mL}$  (b, in Fig. 2A). WSS25 is the sulphated derivative of WGEW (24). However, WGEW showed no inhibitory effect on the tube formation of HMEC-1 cells on Matrigel even at 1 mg/ml (Supplemental file 2). These results indicated that the sulfation indeed contributed to anti-angiogenic effects of WSS25.

Angiogenesis involves multiple steps including migration, proliferation, and capillary tube formation of endothelial cells. Hence, the effects of WSS25 on these phenotypes of HMEC-1 cells were examined. There are two methods to evaluate the migration of endothelial cells, the transwell migration assay and the wound healing assay. We used both of these methods to investigate the effect of WSS25 on the migration of HMEC-1 cells. In the transwell model, WSS25 impaired the migration of HMEC-1 cells (b, c, d in Fig. 2B) in a dose-dependent manner compared with the control (a, in Fig. 2B; Supplemental file 3A). In the wound healing assay (Fig. 2C), the migration of the HMEC-1 cells was also substantially inhibited (Supplemental file 3B) after treatment with 25  $\mu\text{g/mL}$  WSS25 for 48 h (c, in Fig. 2C), compared with the control (d, in Fig. 2C). However, there was no significant effect of

WSS25 on the proliferation of HMEC-1 cells at concentrations less than 100  $\mu\text{g/mL}$  (Fig. 2D).

*Id1 expression is down-regulated in HMEC-1 cells after WSS25 treatment.* As we hypothesised that HS mimetics may inhibit angiogenesis via abrogating BMP induced Id1 expression, an oligo-angiogenesis microarray assay was performed to explore the changes in expression of angiogenic genes including Id1 in HMEC-1 cells after WSS25 treatment. Because WSS25 at 25  $\mu\text{g/mL}$  could nearly completely inhibit the tube formation of HMEC-1 cells on Matrigel, this concentration of WSS25 was used to treat the cells for the microarray analysis. Among the differentially expressed genes (Supplemental file 1), Id1 was the most down-regulated by WSS25 (25  $\mu\text{g/mL}$ ) (red circle in Fig. 3A). This result was further confirmed by RT-PCR (Fig. 3B) and Western blotting analysis (Fig. 3C).

*Id1 expression knock-down in HMEC-1 cells leads to disruption of tube formation on Matrigel.* Since the HS mimetic WSS25 not only inhibited angiogenesis *in vitro* but also blocked Id1 expression in HMEC-1 cells, we wondered if Id1 is truly responsible for the angiogenesis that is inhibited by WSS25. To validate the pro-angiogenic effect of Id1 in HMEC-1 cells, we knocked down expression of Id1 by specific shRNA which indeed led to the disruption of tube formation by the HMEC-1 cells on Matrigel (c, in Fig. 4C) compared with the blank (a, in Fig. 4C) and the sham control (b, in Fig. 4C).

*WSS25 blocks BMP/Smad/Id1 signaling in HMEC-1 cells.* Id1 is the canonical and direct downstream effector of the BMP/Smad pathway (20). Additionally, Id1 expression stimulated by BMP is necessary and sufficient for activation of endothelial cells by BMPs (21). To determine if the inhibition of Id1 expression by WSS25 in HMEC-1 cells was due to the blocking of BMP/Smad signaling, we investigated the impact of WSS25 on the components of this pathway, including BMP2, BMP receptor IA (BMPRIA), BMP receptor IB (BMPRIB), BMP receptor II (BMPRII), and Smad4 in HMEC-1 cells. Interestingly, WSS25 increased the expressions of BMP2 but decreased the expression of BMPRIB and BMPRII (Fig. 5A). However, WSS25 had little effect on the expressions of BMPRIA and Smad4 (Fig. 5A).

BMPs mediate Id1 gene expression via modulating the phosphorylation of Smad1/5/8, which forms a complex with Smad4 after the phosphorylation and then translocates into the

nucleus to modulate Id1 expression. Therefore, we next examined the effect of WSS25 on the phosphorylation of Smad1/5/8 and Id1 expression, both of which are induced by BMP2. Indeed, WSS25 effectively blocked the BMP2 induced phosphorylation of Smad1/5/8 and Id1 expression, similar to the effect of the endogenous BMP2 antagonist noggin used as a control (Fig. 5B). These results indicated that WSS25 down-regulates Id1 expression via inhibition of BMP/Smad signaling in HMEC-1 cells.

*WSS25 binds BMP2 and inhibits BMP2 induced angiogenesis in vitro and in vivo.* Although WSS25 may induce BMP2 expression, the observations above suggested that the blocking of BMP/Smad signaling is sufficient for inhibiting Id1 expression. We then asked whether WSS25 could target BMP2 to block BMP/Smad signaling and inhibit BMP2 induced angiogenesis. Heparin was reported to disrupt BMP/Smad signaling via binding BMPs (30), suggesting that HS mimetics may also bind BMPs and influence their function. Thus, we analyzed the interaction between WSS25 and BMP2 using QCM analysis and found that WSS25 strongly bound to BMP2 (Fig. 6A). This result demonstrated that BMP2 was at least one of the targets of WSS25. Next, we examined the effect of WSS25 on angiogenesis. Indeed, BMP2 could promote angiogenesis in the Matrigel plugged into the C57/BL6 mice (Fig. 6B) and enhance the tube formation of HMEC-1 cells on Matrigel in the FBS restricted condition (b, in Fig. 6C). However, WSS25 could abrogate both the *in vitro* (d, in Fig. 6C) and *in vivo* angiogenic effects of BMP2 (Fig. 6B). Again, as a control and also a BMP2 binding molecule, the endogenous BMP antagonist noggin impaired the tube formation of HMEC-1 cells on Matrigel in this experiment (c, in Fig. 6C). The aforementioned data also suggested that binding to BMP2 conferred WSS25 function as antagonist as noggin did to inhibit the tube formation of HMEC-1 cells.

*WSS25 suppresses the growth of HCC xenografted in nude mice.* Angiogenesis is important for tumor growth, and agents that prevent it can efficiently inhibit tumor growth. As mentioned above, we found that WSS25 could potently disrupt the migration and tube formation of HMEC-1 cells. Based on these observations, WSS25 would theoretically have the potential to inhibit tumor growth via disruption of angiogenesis *in vivo*. Therefore,

two types of HCC cells, Bel7402 and SMMC7721, were subcutaneously inoculated into the front pads of male nude mice (ages ranged 4-6 weeks) to evaluate the effect of WSS25 on tumor growth *in vivo*. WSS25 (100 mg/kg) was administered to the mice via tail vein injection as described in Materials and Methods. The results showed that WSS25 significantly inhibited the growth of both Bel7402 (Fig. 7A) and SMMC7721 (Fig. 7B) cells xenografted into the nude mice. The T/C (%) were 32.2% and 56%, respectively. The result was confirmed by a cell proliferation-associated marker, a ubiquitous nuclear protein Ki-67 staining, since the expression of Ki-67 in the WSS25 treated Bel7402 xenografts was lower than the control (Supplemental file 4, A and B). During the experiments, the body weight of the mice tested showed no significant change in both groups with the xenografts (Fig. 7C and 7D).

*WSS25 inhibits angiogenesis and blocks BMP/Smad/Id1 signaling in HCC xenografted in nude mice.* Since we showed that WSS25 inhibited the growth of HCC xenografted in nude mice, the next question was whether the inhibitory effect of WSS25 on the growth of tumor xenografts could be attributed to attenuation of angiogenesis via inhibition of Id1 expression. To address this question, immunohistochemical analysis was performed to detect the expression of CD31 and Id1 expression in the tumor tissues. CD31 is a well established biomarker in endothelial cells (31), as the micro-vessel density is positively related to its expression. Compared with the control (Fig. 8A), the CD31 expression was significantly lower in the tissue from the WSS25 treated mice (Fig. 8B), suggesting that the angiogenesis was also inhibited *in vivo* by WSS25. Importantly, the expression of Id1 was also down-regulated in the tumor tissue from the mice treated with WSS25 (Fig. 8D). Meanwhile, compared to the control (Fig. 8E), the expression of phosphorylated Smad1/5/8 in tumor tissues (Fig. 8F) after WSS25 treatment was also reduced. These results suggested that the inhibition of tumor growth could be indeed attributed to the inhibition of Id1 expression and subsequent impairment of angiogenesis. Additionally, the Id1 expression inhibition, at least partly, was attributed to the blockade of BMP/Smad signaling.

## DISCUSSION

In this study, we demonstrated that the sulfated glucan WSS25 potently inhibited the tube formation of HMEC-1 cells on Matrigel and migration. However, WSS25 only slightly inhibited the proliferation of the cells at concentrations lower than 100  $\mu\text{g}/\text{mL}$ . The inhibition may be due to the ablation of Id1 expression which could be attributed, at least in part, to the blockade of BMP/Smad signaling. More importantly, WSS25 inhibited angiogenesis and the growth of HCC xenografted in nude mice, while the Id1 expression in the tumor tissue was also substantially down-regulated. Furthermore, WSS25 also blocked the Id1 expression (Supplemental file 5, B and C) and abrogated the BMP/Smad signaling (Supplemental file 6) in Bel7402 cells.

Id1 is well-established as an anti-angiogenesis target. This was also confirmed by our results (Fig. 4). However, it is extremely difficult to directly inhibit Id1 due to its nuclear localization and structural homology to the bHLH transcriptional factors. Although Id1 expression was demonstrated to be effectively inhibited by anti-sense nucleic acids (32, 33), the use of this technology is still not routine in the clinic. Thus, alternative ways to inhibit Id1 are necessary. Id1 is the downstream effector of VEGF (22) and FGF (3). However, both resistance and adverse effect were reported in the US Food and Drug Administration (FDA) approved anti-angiogenesis agents including Sunitinib, Sorafenib, and Bevacizumab, all of which exert their effects via targeting VEGF signalling (34). Id1 was reported to be a common downstream effector of oncogenic tyrosine kinase in leukemic cells (35). Src inhibitor could also impair the expression of Id1 in cancer cells from different sources (36). The Epac/Rap1 related pathway also appears to be the upstream modulator of Id1 (37). However, Id1 is the canonical and direct downstream effector of the BMP/Smad signaling pathway. More importantly, Id1 stimulated by BMPs is sufficient and necessary for the activation of endothelial cells by BMPs (21). Thus, blocking BMP/Smad signaling is an ideal choice for inhibiting Id1 expression.

Accumulating evidences have demonstrated that BMP proteins are involved in angiogenesis regulation. The well-established examples include BMP2 and BMP4. BMP2 was found to promote the tumor angiogenesis of non-small

lung cancer cell in nude mice (38,39). Both BMP2 and BMP4 were reported to enhance angiogenesis in melanoma tumors (40). The angiogenic effect was exerted through the signaling triggered through the BMP type I receptor (BMPRIA, BMPRIB) and BMP type II receptor (BMPRII). Their co-receptor betaglycan (type III TGFbeta receptor), which is a proteoglycan, also plays an important role in the signal transduction process (18). Additionally, Id1 expression stimulated by BMP proteins was sufficient and necessary for activation of endothelial cells (21). More importantly, BMPRII was demonstrated to be required for maintenance of vascular integrity (41). In our study, BMP2, BMPRIA, BMPRIB, and BMPRII were all expressed in the HMEC-1 cells (Fig. 5A). Both the expression of Id1 and the phosphorylation of Smad1/5/8 induced by BMP2 were inhibited by WSS25 (Fig. 5B). Although the expression of BMP2 was up-regulated after 18 h of treatment with WSS25, the overall effects of WSS25 treatment was the blockade of BMP/Smad signaling. Furthermore, the expression of BMP2 was increased only by WSS25 after 18 h of treatment (Supplemental file 7). In addition to the BMP blocking effect, the overall effects of WSS25 could be partly due to the down-regulation of BMPRIB and BMPRII, since BMPRIB overexpressed by plasmid transfection into the HMEC-1 cells could partially rescue the inhibition of tube formation by WSS25 treatment (Supplemental file 8).

HS mimetics are widely reported to inhibit angiogenesis through blocking the interaction between the angiogenic factors and their receptors. The most frequently reported angiogenic factors are FGF2 and VEGF. For example, the HS mimetic PI-88, which is in Phase II clinical trials for several types of cancer (42), inhibits angiogenesis by strongly binding to FGF1, FGF2, and VEGF (15,43). HS was also reported to bind to the BMP proteins to interfere with BMP/Smad signaling. For example, heparin could bind with BMP2 proteins as demonstrated by QCM (30) and surface plasmon resonance (SPR) (16) analysis. This interaction would lead to the blocking of BMP/Smad signaling. WSS25, as a sulfated derivative of an alpha-D-glucan and a HS mimetic, could strongly bind with the BMP2 protein (Fig. 6A) and block the BMP/Smad signaling as heparin did. Furthermore, WSS25 inhibited BMP2 induced angiogenesis *in vitro* and *in vivo*. Thus, these findings could reasonably explain the down-

regulation of Id1 and inhibition of angiogenesis and HCC growth by WSS25. Moreover, heparin was reported to bind to the BMP receptors, BMPRIA, BMPRIB, and BMPRII. Since WSS25 is structurally similar to heparin and glycosaminoglycan chains attached to the core protein of betaglycan, we therefore speculated that WSS25 may also bind with the BMP receptors to block the activation of the BMP/Smad signaling. Recently, BMP2 was reported to induce angiogenesis through non-canonical pathways such as the Wnt/beta-catenin and Wnt/RhoA/Rac1 pathways (44). As mentioned earlier, WSS25 can tightly bind with BMP2, and this interaction may also lead to inhibition of the non-canonical angiogenic signals by blocking the activation by BMP2. Although WSS25 was found to strongly bind with BMP2, the exact structural domain required for the binding is still not clear and remains to be determined in future work.

Id1 is the downstream effector of VEGF (22) and FGF (3). HS could bind with VEGF and

FGF to modulate angiogenesis. Thus, WSS25 may inhibit Id1 expression through disrupting the interaction between them, although this hypothesis needs to be confirmed by further work. Over-expression of Id1 in HCC cells induces cell proliferation (10). Accordingly, the inhibitory effect of WSS25 on the growth of HCC xenografted in nude mice could also be attributed to the direct inhibition of the HCC cell growth, while only slightly inhibited the proliferation of HCC cells (Supplemental file 2A).

In summary, we reported here that WSS25, a HS mimetic, inhibited the growth of HCC xenografted in nude mice via disruption of angiogenesis by abrogating Id1 expression. This inhibition of Id1 expression was due, at least partly, to the blocking of BMP/Smad signaling. Thus WSS25 is a potential drug candidate for HCC therapy that would function via blockade of Id1 expression.

## REFERENCES

1. Tang, Z. Y. (2001) *World J Gastroenterol* **7**, 445-454
2. Sun, H. C., and Tang, Z. Y. (2004) *J Cancer Res Clin Oncol* **130**, 307-319
3. Perk, J., Iavarone, A., and Benezra, R. (2005) *Nat Rev Cancer* **5**, 603-614
4. Ouyang, X. S., Wang, X., Lee, D. T., Tsao, S. W., and Wong, Y. C. (2002) *J Urol* **167**, 2598-2602
5. Perk, J., Gil-Bazo, I., Chin, Y., de Candia, P., Chen, J. J., Zhao, Y., Chao, S., Cheong, W., Ke, Y., Al-Ahmadie, H., Gerald, W. L., Brogi, E., and Benezra, R. (2006) *Cancer Res* **66**, 10870-10877
6. Lyden, D., Young, A. Z., Zagzag, D., Yan, W., Gerald, W., O'Reilly, R., Bader, B. L., Hynes, R. O., Zhuang, Y., Manova, K., and Benezra, R. (1999) *Nature* **401**, 670-677
7. Ruzinova, M. B., Schoer, R. A., Gerald, W., Egan, J. E., Pandolfi, P. P., Rafii, S., Manova, K., Mittal, V., and Benezra, R. (2003) *Cancer Cell* **4**, 277-289
8. Lyden, D., Hattori, K., Dias, S., Costa, C., Blaikie, P., Butros, L., Chadburn, A., Heissig, B., Marks, W., Witte, L., Wu, Y., Hicklin, D., Zhu, Z., Hackett, N. R., Crystal, R. G., Moore, M. A., Hajar, K. A., Manova, K., Benezra, R., and Rafii, S. (2001) *Nat Med* **7**, 1194-1201
9. Ling, M. T., Wang, X., Zhang, X., and Wong, Y. C. (2006) *Differentiation* **74**, 481-487
10. Lee, T. K., Man, K., Ling, M. T., Wang, X. H., Wong, Y. C., Lo, C. M., Poon, R. T., Ng, I. O., and Fan, S. T. (2003) *Carcinogenesis* **24**, 1729-1736
11. Lee, T. K., Poon, R. T., Yuen, A. P., Ling, M. T., Wang, X. H., Wong, Y. C., Guan, X. Y., Man, K., Tang, Z. Y., and Fan, S. T. (2006) *Clin Cancer Res* **12**, 6910-6919
12. Iozzo, R. V., and San Antonio, J. D. (2001) *J Clin Invest* **108**, 349-355
13. Ding, K., Lopez-Burks, M., Sanchez-Duran, J. A., Korc, M., and Lander, A. D. (2005) *J Cell Biol* **171**, 729-738
14. Esko, J. D., and Selleck, S. B. (2002) *Annu Rev Biochem* **71**, 435-471
15. Karoli, T., Liu, L., Fairweather, J. K., Hammond, E., Li, C. P., Cochran, S., Bergefall, K., Trybala, E., Addison, R. S., and Ferro, V. (2005) *J Med Chem* **48**, 8229-8236
16. Ruppert, R., Hoffmann, E., and Sebald, W. (1996) *Eur J Biochem* **237**, 295-302
17. Ohkawara, B., Iemura, S., ten Dijke, P., and Ueno, N. (2002) *Curr Biol* **12**, 205-209
18. David, L., Feige, J. J., and Bailly, S. (2009) *Cytokine Growth Factor Rev* **20**, 203-212
19. Rider, C. C. (2006) *Biochem Soc Trans* **34**, 458-460
20. Miyazono, K., and Miyazawa, K. (2002) *Sci STKE* **2002**, pe40
21. Valdinarsdottir, G., Goumans, M. J., Rosendahl, A., Brugman, M., Itoh, S., Lebrin, F., Sideras, P., and ten Dijke, P. (2002) *Circulation* **106**, 2263-2270
22. Sakurai, D., Tsuchiya, N., Yamaguchi, A., Okaji, Y., Tsuno, N. H., Kobata, T., Takahashi, K., and Tokunaga, K. (2004) *J Immunol* **173**, 5801-5809
23. Lindahl, U. (2007) *Thromb Haemost* **98**, 109-115
24. Qiu, H., Tang, W., Tong, X., Ding, K., and Zuo, J. (2007) *Carbohydr Res* **342**, 2230-2236
25. Xu, Y., Swerlick, R. A., Sepp, N., Bosse, D., Ades, E. W., and Lawley, T. J. (1994) *J Invest Dermatol* **102**, 833-837
26. Peddada, S., Yasui, D. H., and LaSalle, J. M. (2006) *Hum Mol Genet* **15**, 2003-2014
27. McAllister, S. D., Christian, R. T., Horowitz, M. P., Garcia, A., and Desprez, P. Y. (2007) *Mol Cancer Ther* **6**, 2921-2927
28. Cejalvo, T., Sacedon, R., Hernandez-Lopez, C., Diez, B., Gutierrez-Frias, C., Valencia, J., Zapata, A. G., Varas, A., and Vicente, A. (2007) *Immunology* **121**, 94-104
29. Folkman, J., and Haudenschild, C. (1980) *Nature* **288**, 551-556
30. Kanzaki, S., Takahashi, T., Kanno, T., Ariyoshi, W., Shinmyozu, K., Tujisawa, T., and Nishihara, T. (2008) *J Cell Physiol* **216**, 844-850
31. Jia, J., Wang, J., Teh, M., Sun, W., Zhang, J., Kee, I., Chow, P. K., Liang, R. C., Chung, M. C., and Ge, R. (2009) *Proteomics*
32. Fong, S., Itahana, Y., Sumida, T., Singh, J., Coppe, J. P., Liu, Y., Richards, P. C., Bennington, J. L., Lee, N. M., Debs, R. J., and Desprez, P. Y. (2003) *Proc Natl Acad Sci U S A* **100**, 13543-13548

33. Henke, E., Perk, J., Vider, J., de Candia, P., Chin, Y., Solit, D. B., Ponomarev, V., Cartegni, L., Manova, K., Rosen, N., and Benezra, R. (2008) *Nat Biotechnol* **26**, 91-100
34. Bergers, G., and Hanahan, D. (2008) *Nat Rev Cancer* **8**, 592-603
35. Tam, W. F., Gu, T. L., Chen, J., Lee, B. H., Bullinger, L., Frohling, S., Wang, A., Monti, S., Golub, T. R., and Gilliland, D. G. (2008) *Blood* **112**, 1981-1992
36. Gautschi, O., Tepper, C. G., Purnell, P. R., Izumiya, Y., Evans, C. P., Green, T. P., Desprez, P. Y., Lara, P. N., Gandara, D. R., Mack, P. C., and Kung, H. J. (2008) *Cancer Res* **68**, 2250-2258
37. Doebele, R. C., Schulze-Hoepfner, F. T., Hong, J., Chlenski, A., Zeitlin, B. D., Goel, K., Gomes, S., Liu, Y., Abe, M. K., Nor, J. E., Lingen, M. W., and Rosner, M. R. (2009) *Blood*
38. Langenfeld, E. M., and Langenfeld, J. (2004) *Mol Cancer Res* **2**, 141-149
39. Raida, M., Clement, J. H., Leek, R. D., Ameri, K., Bicknell, R., Niederwieser, D., and Harris, A. L. (2005) *J Cancer Res Clin Oncol* **131**, 741-750
40. Rothhammer, T., Bataille, F., Spruss, T., Eissner, G., and Bosserhoff, A. K. (2007) *Oncogene* **26**, 4158-4170
41. Liu, D., Wang, J., Kinzel, B., Mueller, M., Mao, X., Valdez, R., Liu, Y., and Li, E. (2007) *Blood* **110**, 1502-1510
42. Ferro, V., Dredge, K., Liu, L., Hammond, E., Bytheway, I., Li, C., Johnstone, K., Karoli, T., Davis, K., Copeman, E., and Gautam, A. (2007) *Semin Thromb Hemost* **33**, 557-568
43. Parish, C. R., Freeman, C., Brown, K. J., Francis, D. J., and Cowden, W. B. (1999) *Cancer Res* **59**, 3433-3441
44. de Jesus Perez, V. A., Alastalo, T. P., Wu, J. C., Axelrod, J. D., Cooke, J. P., Amieva, M., and Rabinovitch, M. (2009) *J Cell Biol* **184**, 83-99

## FOOTNOTES

§ These authors contributed equally to this work. \*The work is supported by grants from the National Natural Science Foundation of China (Grant No. 30670470); the National High Technology Research and Development Program (863) of China (Grant No. 2006AA022102); New Drug Research Program of the Shanghai Institute of Materia Medica, Chinese Academy of Sciences (Grant No. 07G604F036); ‘100 Talents Project’ of Chinese Academy of Sciences, China (Professor Kan Ding); Knowledge Innovation Program of Chinese Academy of Sciences (Grant No. KSCX1-YW-R-18); and the National Science & Technology Major Project “Key New Drug Creation and Manufacturing Program” (2009ZX09301-001, 2009ZX09103-071). We thank Mr. Shengguang Fu in Shanghai University of Traditional Chinese Medicine for the great assistance in animal study. We also thank other members in the lab for their critical comments on the manuscript.

## FIGURE LEGENDS

**Fig. 1.** Structural diagram of WSS25.

**Fig. 2.** WSS25 impaired the tube formation of HMEC-1 cells on Matrigel and migration. A, WSS25 inhibited the tube formation of HMEC-1 cells on Matrigel. HMEC-1 cells (90  $\mu$ L) treated with WSS25 (10  $\mu$ L) at different final concentrations (b, 6.25  $\mu$ g/mL; c, 25  $\mu$ g/mL; d, 50  $\mu$ g/mL) or vehicle (a) were seeded into the 96-well plate pre-coated with 50  $\mu$ L matrigel for 10 h. B, WSS25 impaired the migration of HMEC-1 cells in a transwell migration assay. HMEC-1 cells were seeded into the inner chamber with MCDB131 medium containing 10  $\mu$ g/mL (b), 100  $\mu$ g/mL (c), 1 mg/mL WSS25 (d) or vehicle (a). C, WSS25 inhibited the migration of HMEC-1 cells in a wound healing assay (a and c, control; b and d, 25  $\mu$ g/mL). D, HMEC-1 cells were seeded into the 96-well plate. After 24 h incubation, WSS25 was added to the final concentrations of 1  $\mu$ g/mL, 10  $\mu$ g/mL, 100  $\mu$ g/mL, 500  $\mu$ g/mL or 1 mg/mL. The cell viabilities were determined by the MTT assay 24 h (☒), 48 h (☑), or 72 h (☐) later. The results are representative of triplicate experiments.

**Fig. 3.** WSS25 potently inhibited the expression of Id1. A, HMEC-1 cells were treated with WSS25 (25  $\mu\text{g}/\text{mL}$ ) for 18 h. RNA was then extracted for the oligo-angiogenesis microarray analysis. The red circle indicates Id1. B, WSS25 at 25  $\mu\text{g}/\text{mL}$  nearly completely inhibited the Id1 mRNA expression in HMEC-1 cells with 18S rRNA as the internal control. C, WSS25 down-regulated the Id1 protein expression in HMEC-1 cells in a dose-dependent manner.  $\beta$ -actin was used as a control for protein loading. Except for the microarray analysis, all experiments were repeated three times.

**Fig. 4.** Id1 knock-down in HMEC-1 cells caused disruption of tube formation on Matrigel. A and B, HMEC-1 cells were plated into 6-well plates for 24 h before transfection with Id1 shRNA for 30 h. Both RT-PCR and Western blotting were then used to detect Id1 expression. Id1 shRNA could downregulate Id1 expression at mRNA level (Fig. 4A) and protein level (Fig. 4B). C, The tube formation of HMEC-1 cells on matrigel was disrupted (c) after Id1 shRNA transfection, compared to the blank (a) and sham control (b). HMEC-1 cells ( $2.5 \times 10^5$  cells/well) were seeded into a 6-well plate for 24 h before transfection. The shRNA plasmids were transfected into the cells three times 24 h apart using X-fect polymer (Clontech, U.S.A.). The cells were used in the tube formation assay according to the Methods 24 h after the last transfection. Photos were taken after another 12 h of incubation. The results are representative of three experiments.

**Fig. 5.** Effects of WSS25 on Id1, BMP2 and Smad signaling pathway components. A, WSS25 displayed different effects on the expressions of BMP2, BMPRIA, BMPRIB, BMPRII, and Smad4. RT-PCR analysis was performed as described in Materials and Methods. B, WSS25 or noggin inhibited both Smad1/5/8 phosphorylation and Id1 expression in HMEC-1 cells induced by BMP2. The cells were pre-treated with 25  $\mu\text{g}/\text{mL}$  of WSS25, 5  $\mu\text{g}/\text{mL}$  noggin or vehicle for 23 h. The cells were then treated with 50 ng/mL of BMP2 or vehicle for another hour. The extracted proteins were analyzed by Western blotting using Id1, Smad1, and pSmad1/5/8 antibodies. The  $\beta$ -actin was used as a control for protein loading. The experiments were repeated twice.

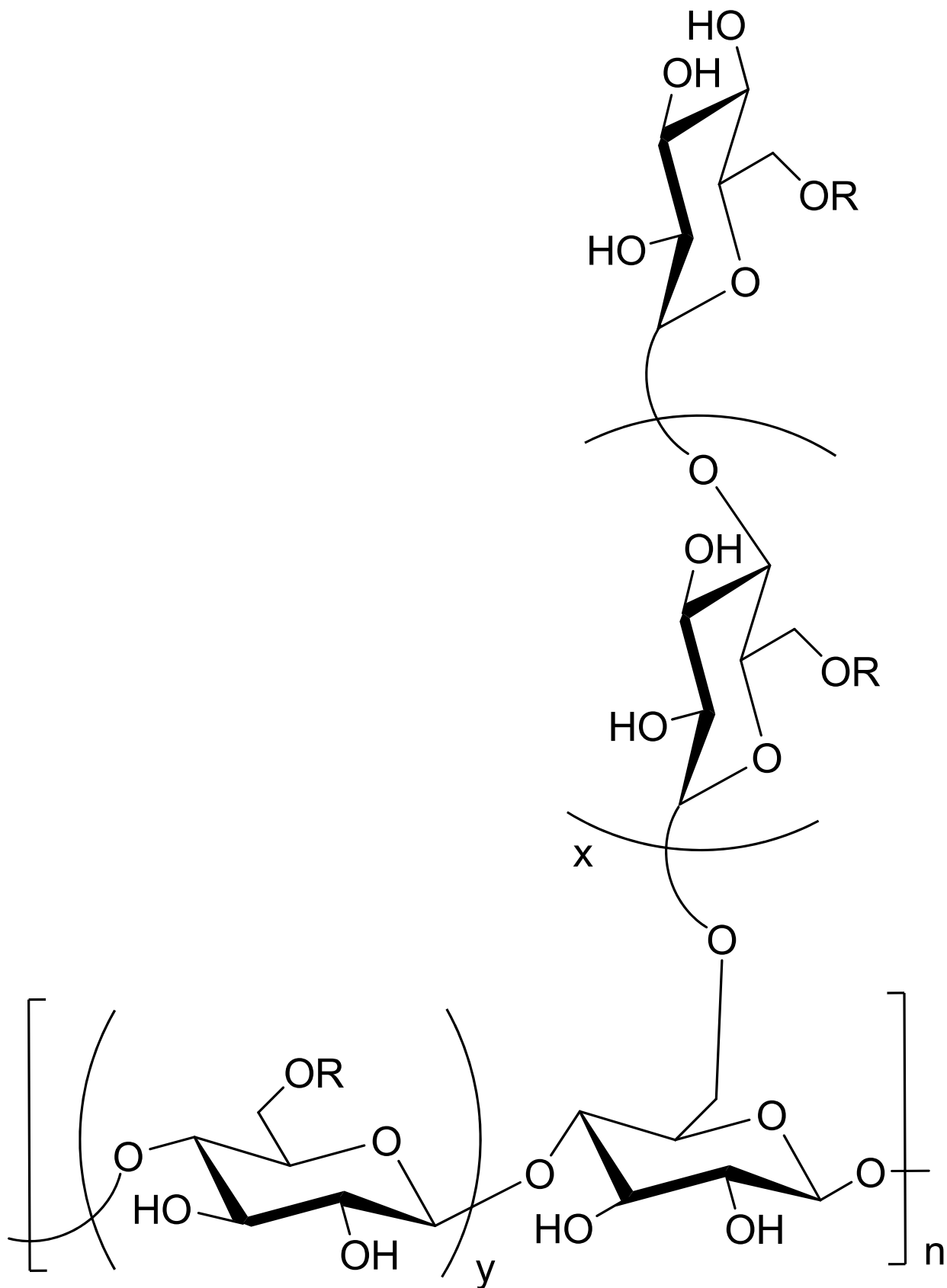
**Fig. 6.** Interaction of WSS25 with BMP2 and its effects on BMP2 induced angiogenesis. A, WSS25 strongly bound to BMP2 by QCM analysis. The WSS25 biosensor surface was prepared for measuring carbohydrate-protein interactions, where the frequency shift produced from biotinylated WSS25 binding to the streptavidin surface is shown in (a). The WSS25-BMP2 interaction was tested by injecting BMP2 (50  $\mu\text{g}/\text{mL}$ , 50  $\mu\text{L}$ ) in running buffer onto the WSS25 biosensor surface, and the frequency response is displayed in (b) (blue curve). The large shift produced indicated that WSS25 bound to BMP2 strongly. As a control, the frequency responses by the BMP2 interaction with the streptavidin surface were measured, yielding a small response in (b) (the pink curve). These results indicate the BMP2-WSS25 interaction was specific. B, WSS25 inhibited BMP2 induced angiogenesis in the Matrigel plug assay. Matrigel (500  $\mu\text{L}$ ) with or without BMP2 (4  $\mu\text{g}/\text{mL}$ ) was subcutaneously injected into the ventral region of C57/BL6 mice. WSS25 (25 mg/kg or 100 mg/kg body weight) was administered to the mice every other day from the second day after the Matrigel was plugged into the mice. Normal saline was used as the control. C, WSS25 and noggin inhibited BMP2 induced tube formation of HMEC-1 cells on Matrigel. Growth factor reduced Matrigel (50  $\mu\text{L}$  per well) was added to a 96-well plate to be solidified in 37°C for 30 min. HMEC-1 cells ( $3 \times 10^4$  cells in 98  $\mu\text{L}$  MCDB131 medium supplemented with 0.1% FBS per well) were seeded into the 96-well plate after the Matrigel solidification. BMP2 (200 ng/mL) was added together with the cells only (b), or in the presence of noggin (1  $\mu\text{g}/\text{mL}$ ) (c) or WSS25 (25  $\mu\text{g}/\text{mL}$ ) (d). Photos were taken after incubation for 24 h at 37°C.

**Fig. 7.** WSS25 represses the growth of HCC xenografted in nude mice. Bel7402 cells (A) and SMMC7721 cells (B) were subcutaneously injected into the front pad of male nude mice. For the Bel7402 xenografts (5 mice/group), after the tumor volume grew to  $\sim 100 \text{ mm}^3$ , 100 mg/kg of WSS25 in normal saline or the vehicle were injected via tail vein every other day. For the SMMC7721 xenografts, well-developed tumors were cut into 1-3  $\text{mm}^3$  fragments and transplanted subcutaneously into the right flank of the nude mice using a trocar under sterile conditions. When the tumor volume reached  $\sim 100 \text{ mm}^3$ , the mice were randomly assigned into control and treatment groups

(6 mice / group), and the vehicle or 100 mg/kg WSS25 was administered via tail vein every other day. Tumor volume was measured using a caliber on the indicated days. Mice were sacrificed 22 days after treatment. The therapeutic effect of the compounds was expressed as the volume ratio of treatment to control (T/C).  $T/C (\%) = 100\% \times (\text{mean RTV of the treated group} / \text{mean RTV of the control group})$ . The tumor growth was significantly inhibited in both tumor models. \*  $P < 0.05$ ; \*\*  $P < 0.01$ . The T/C (%) for Bel7402 and SMMC7721 was 32.2% and 56%, respectively. The mice body weights showed no significant changes during the experiments.

**Fig. 8.** Id1, phosphorylated Smad1/5/8, and CD31 expression levels were lower in WSS25 treated tumor tissue than in the control. Immunohistochemical analysis was performed on tumors from mice treated with 100 mg/kg of WSS25 via tail vein injection or the vehicle as described above. Compared with the control (A), there was also a reduction in the number of blood vessels (shown by reduced expression of the CD31 endothelial marker) in tumors treated with 100 mg/kg WSS25 (B) as indicated by the arrow. Representative images showed that treatment with WSS25 down-regulated Id1 expression in the tumor tissue (C) compared with the control (D) as indicated by the arrow. Phosphorylated Smad1/5/8 expression was also reduced in the WSS25 treated tissues (F) compared to the control (E). All images are at  $400 \times$  magnification.

# Figure 1



WSS25  $\text{R}=\text{SO}$  or  $\text{H}$  ( $x+y=16$ )

Figure 2

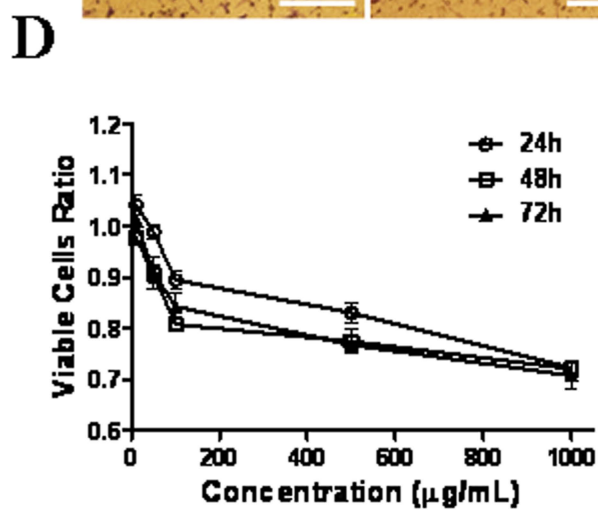
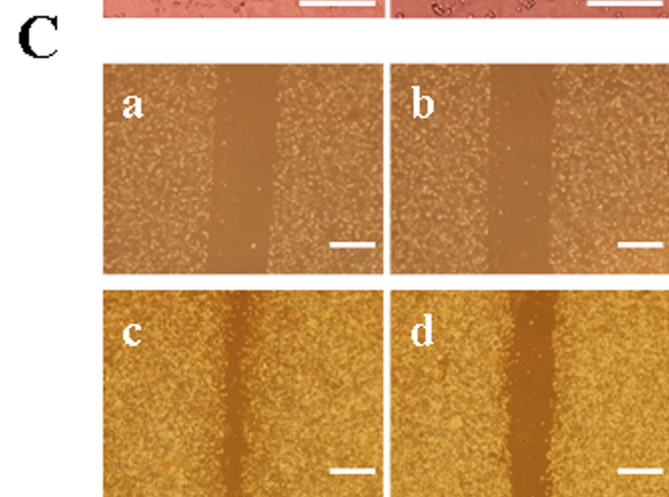
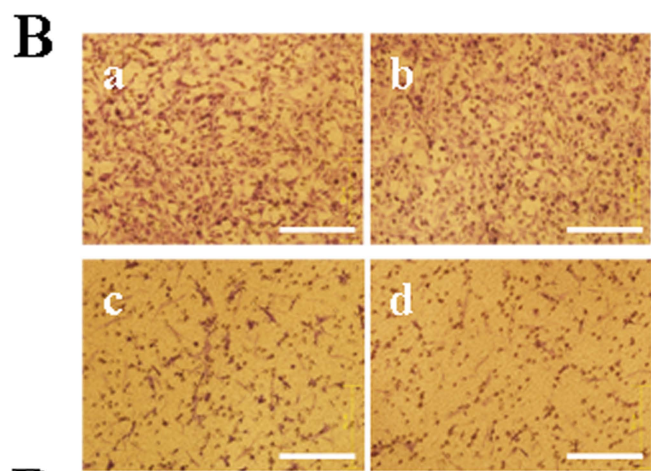
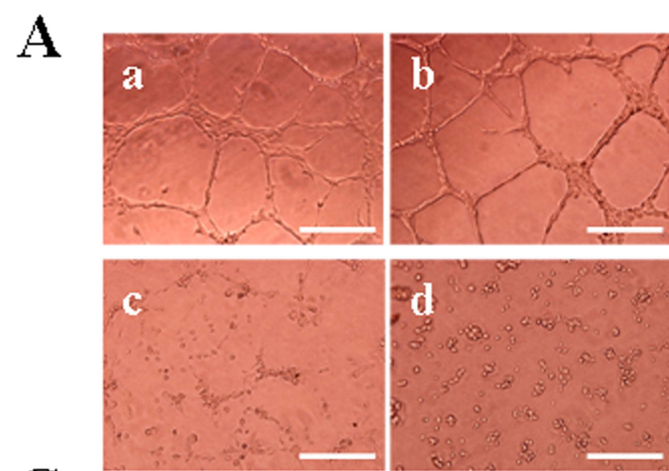


Figure 3

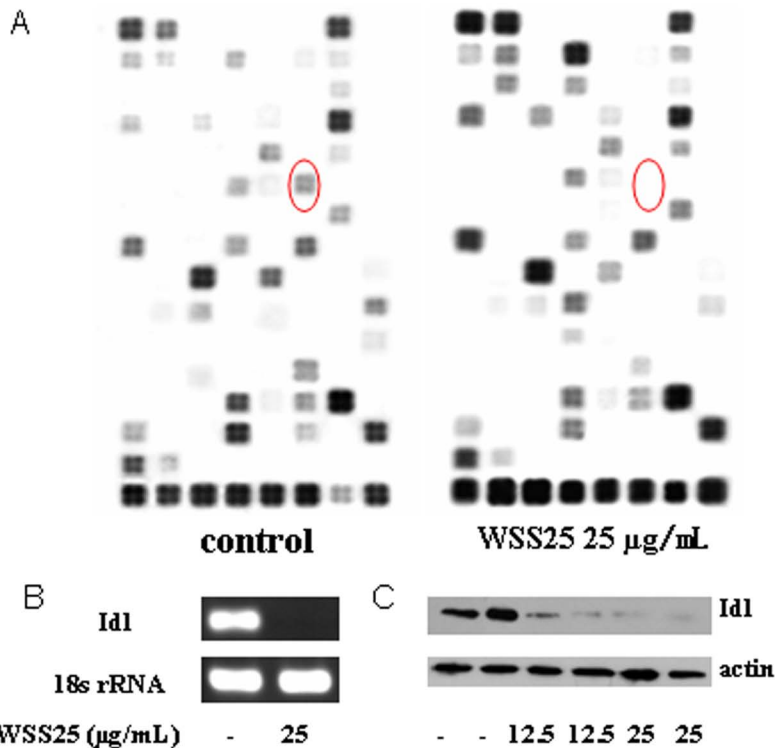
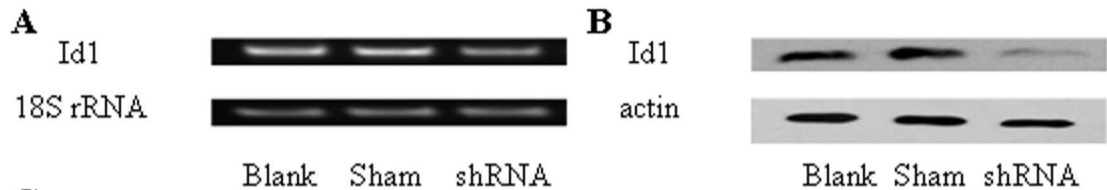


Figure 4



**C**

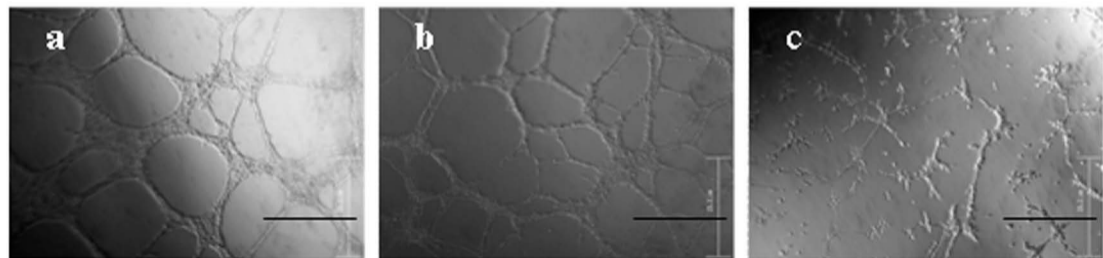


Figure 5

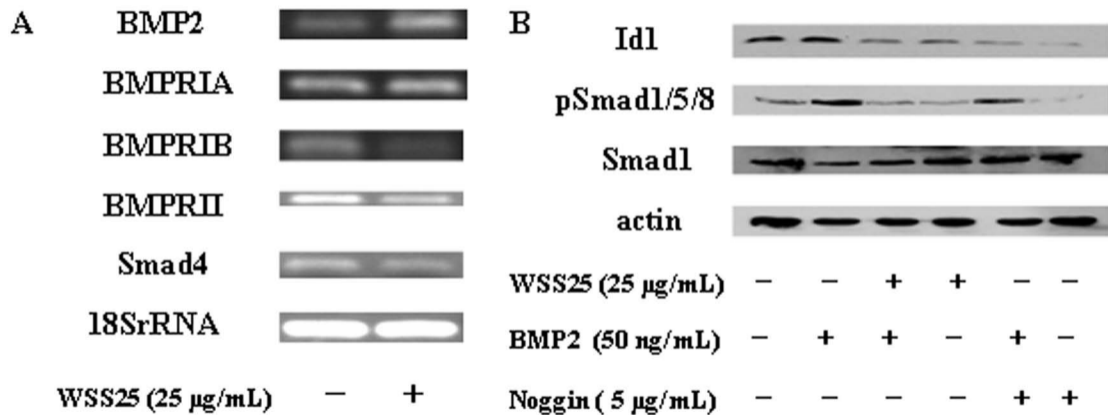
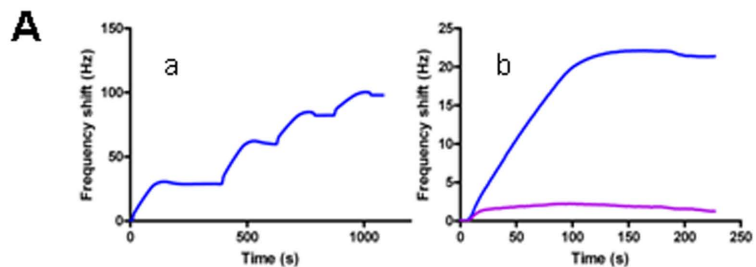


Figure 6



**B**



|                                   |   |   |    |     |
|-----------------------------------|---|---|----|-----|
| BMP2 (4 $\mu\text{g}/\text{mL}$ ) | - | + | +  | +   |
| WSS25 (mg/kg)                     | - | - | 25 | 100 |

**C**

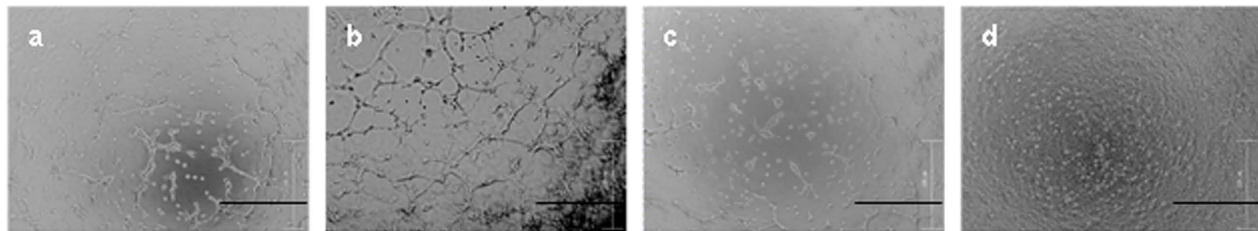
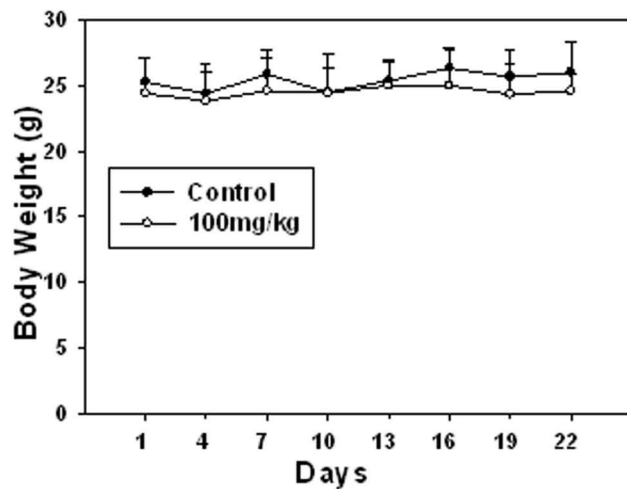
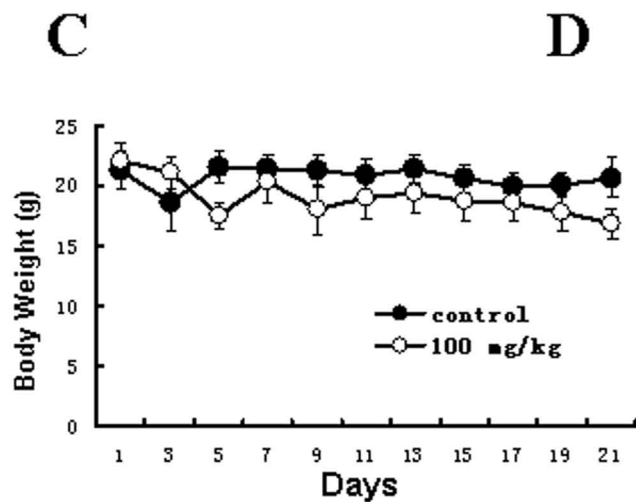
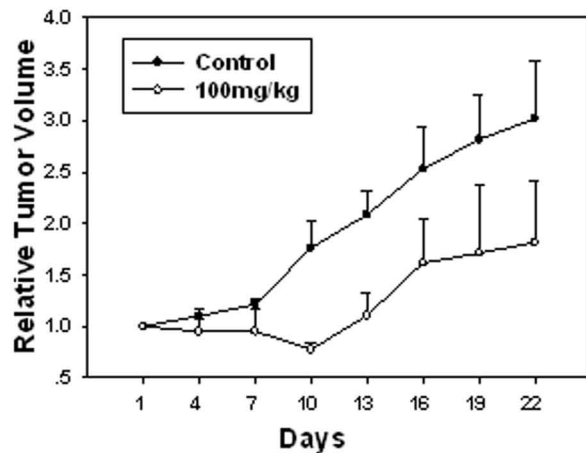
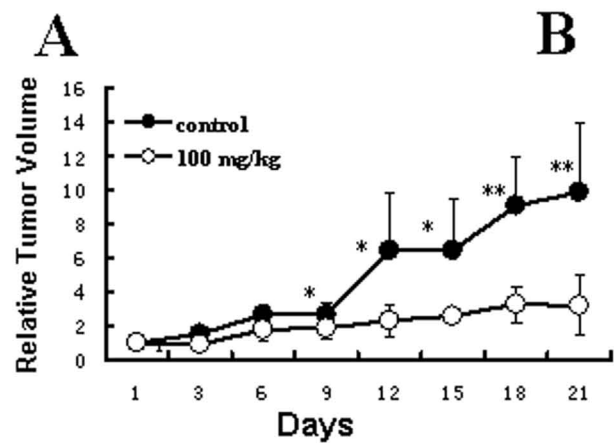
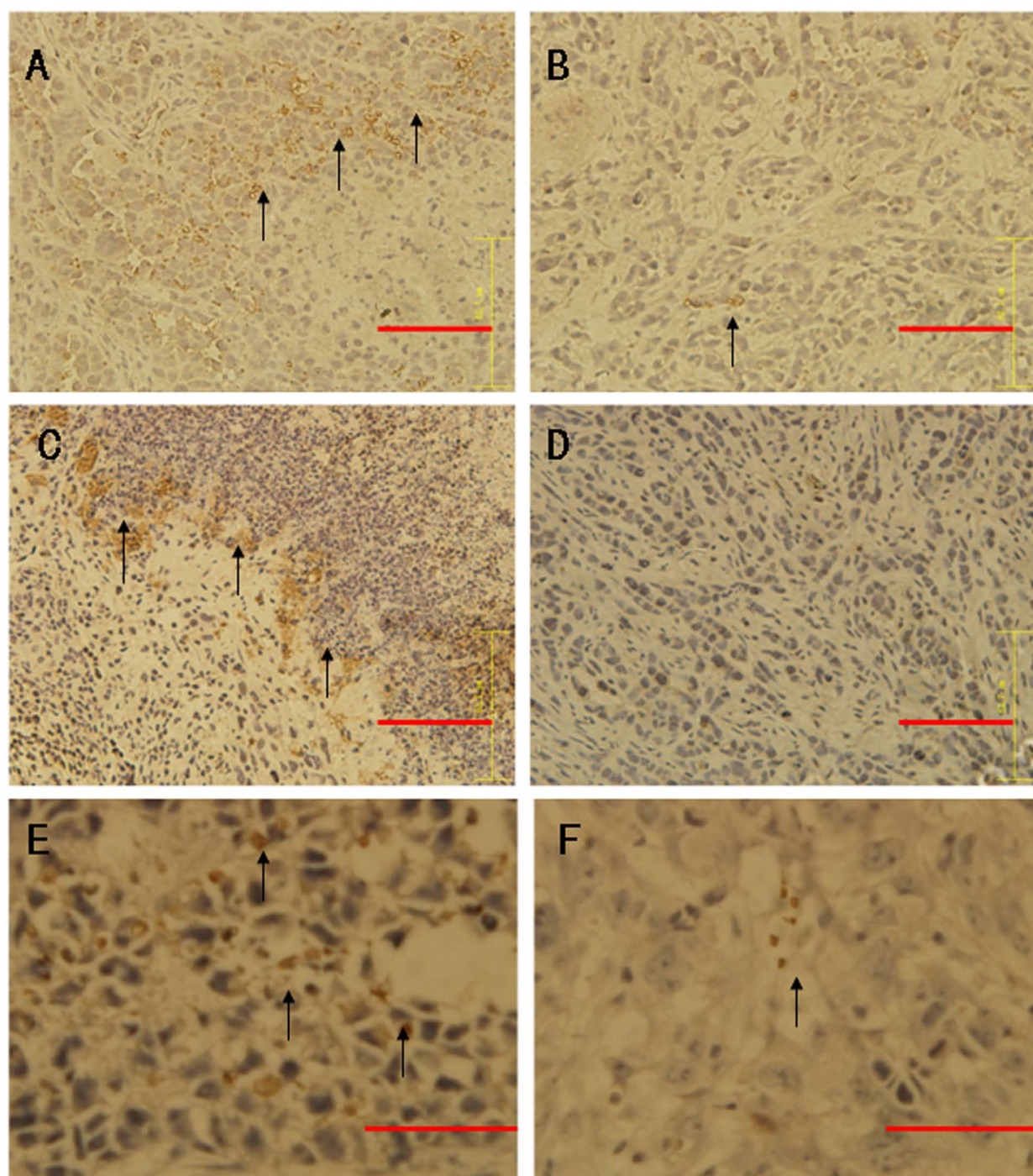


Figure 7



**Figure 8**



**control**

**100 mg/kg WSS25**